Supplementary Information

Significant contrasts in aerosol acidity between China and the Unites States

Bingqing Zhang[1], Huizhong Shen[1], Pengfei Liu[2], Hongyu Guo[3], Yongtao Hu[1], Yilin Chen[1], Shaodong Xie[4], Ziyan Xi[4], Armistead G. Russell[1]

[1]School of Civil and Environmental Engineering, Georgia Institute of Technology, Atlanta, Georgia 30332, USA

[2]School of Earth and Atmospheric Sciences, Georgia Institute of Technology, Atlanta, Georgia 30332, USA

[3]Cooperative Institute for Research in Environmental Sciences and Department of Chemistry, University of Colorado, Boulder, Colorado 80309, USA

[4]College of Environmental Sciences and Engineering, State Key Joint Laboratory of Environmental Simulation and Pollution Control, Peking University, Beijing, 100871, PR China

Correspondence to: Huizhong Shen (hshen73@gatech.edu)

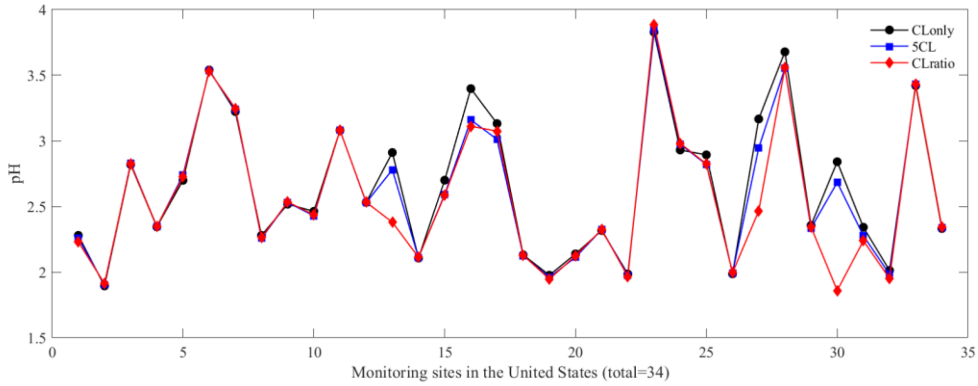

Figure S1: Comparison of results in pH calculation when using different methods to estimate HCl concentration in the United States. Group "Cl only" means using particle Cl^- concentration as total Cl and ignore gas phase HCl; group "5Cl" means assuming total Cl equals to 5 times particle Cl^- concentration therefore HCl concentration equals to 4 times particle Cl^- concentration; group "Cl ratio" means using measured particle $Cl^=$ concentration divided by CMAQ simulation partitioning ratio to estimate the amount of total Cl. The result showed the three methods will lead to essentially the same pH at most of the monitoring sites.

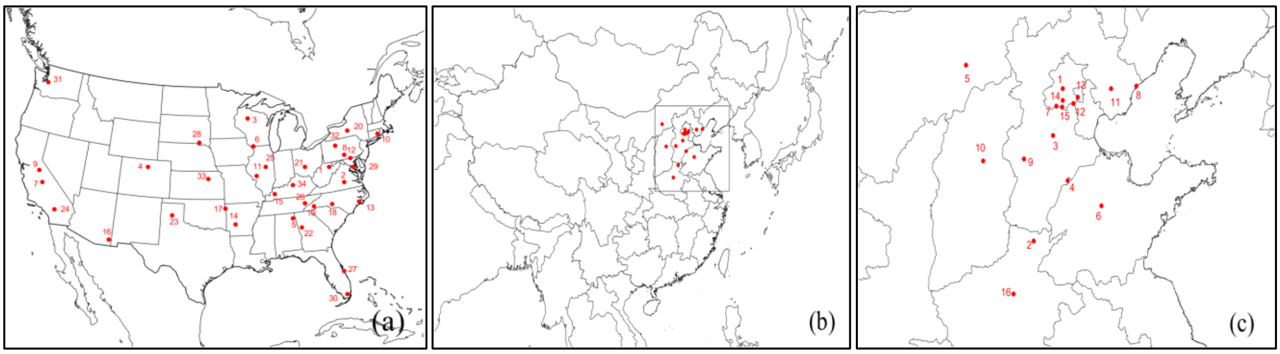

Figure S2: Location of monitoring sites used in this study in the United States(a) and China(b), with a close-up of North China Plain (c).

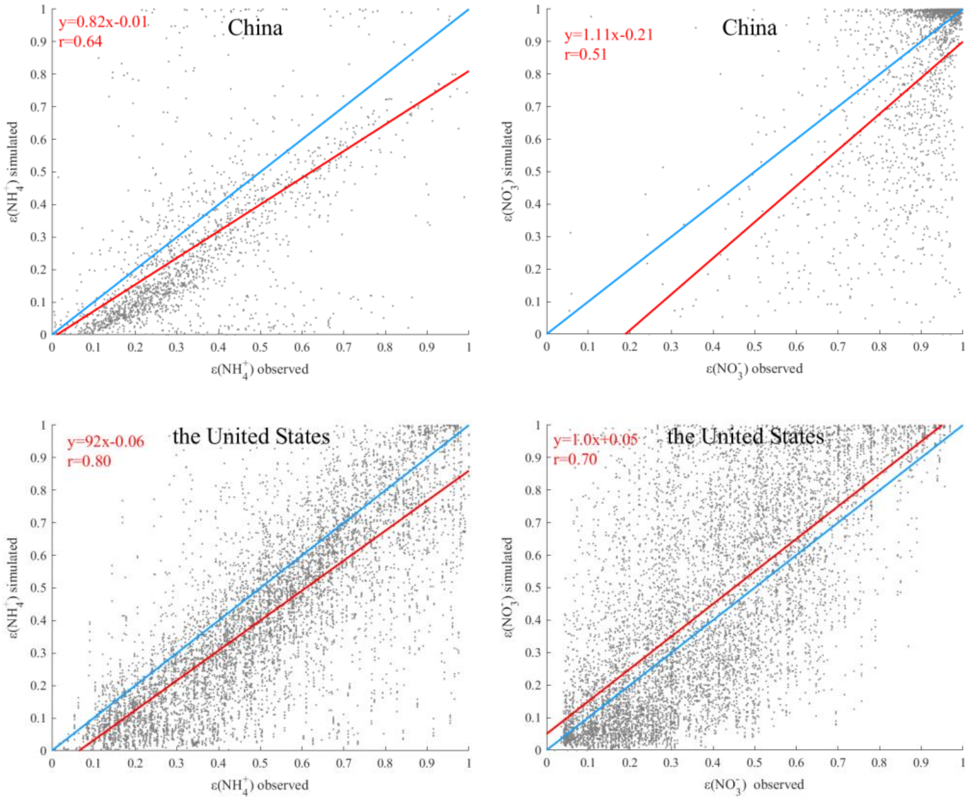

Figure S3: Observed ε(NH_4^+) (left column) and ε(NO_3^-) (right column) in China (top row) and the United States (bottom row) versus simulated by ISORROPIA-II. The regression line(red), 1:1 line(blue), and the regression equation and correlation coefficient r are shown on each panel.

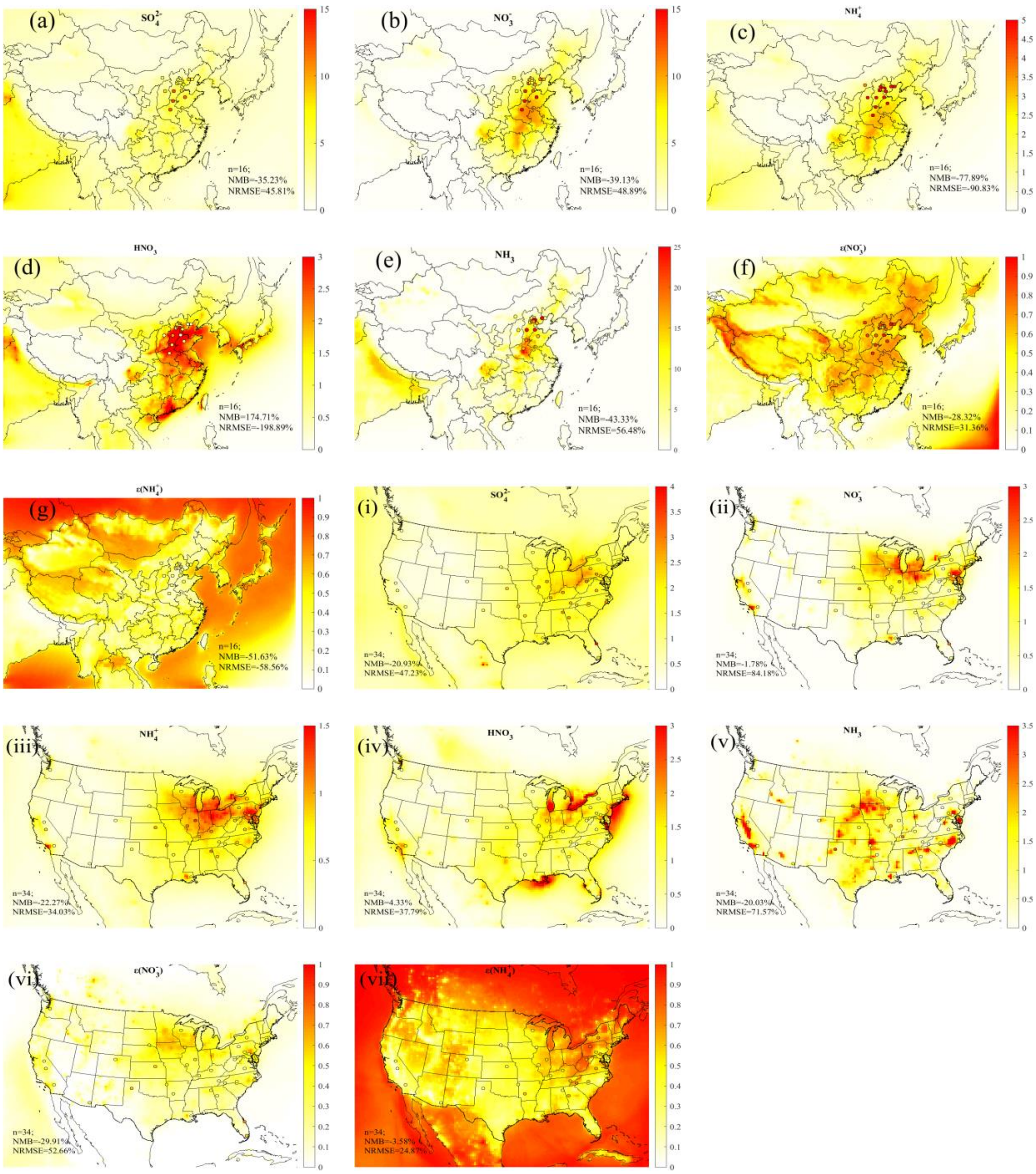

Figure S4: Annual mean concentrations of $PM_{2.5}$ components SO_4^{2-}, NO_3^-, NH_4^+, gaseous components HNO_3 and NH_3 and the partitioning including $\varepsilon(NO_3^-)$ and $\varepsilon(NH_4^+)$ based on CMAQ simulations (colored map) and observations (colored dots) in China (panels a-g) and in the United States (panels i-vii). Normalized mean bias (NMB) and normalized root mean square error (NRMSE) are shown on each panel.

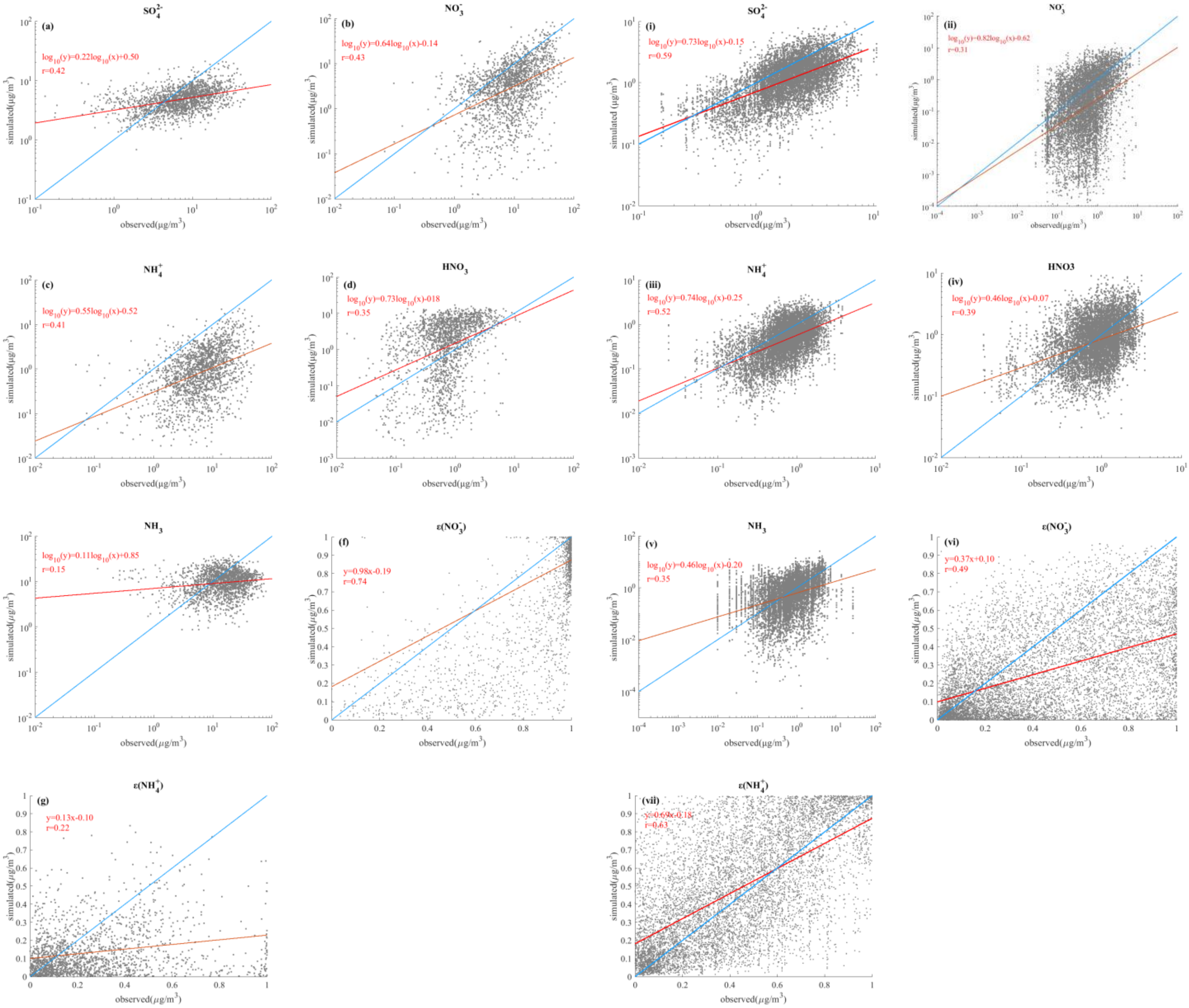

Figure S5: Comparison of daily observed and CMAQ simulated aerosol component concentrations of SO_4^{2-}, NO_3^-, NH_4^+, gaseous concentrations of HNO_3 and NH_3 and the partitioning $\varepsilon(NO_3^-)$ and $\varepsilon(NH_4^+)$ in China (panels a-g) and in the United States (panels i-vii). The regression line (red), 1:1 line (blue), regression equation and correlation coefficient r are shown in each panel.

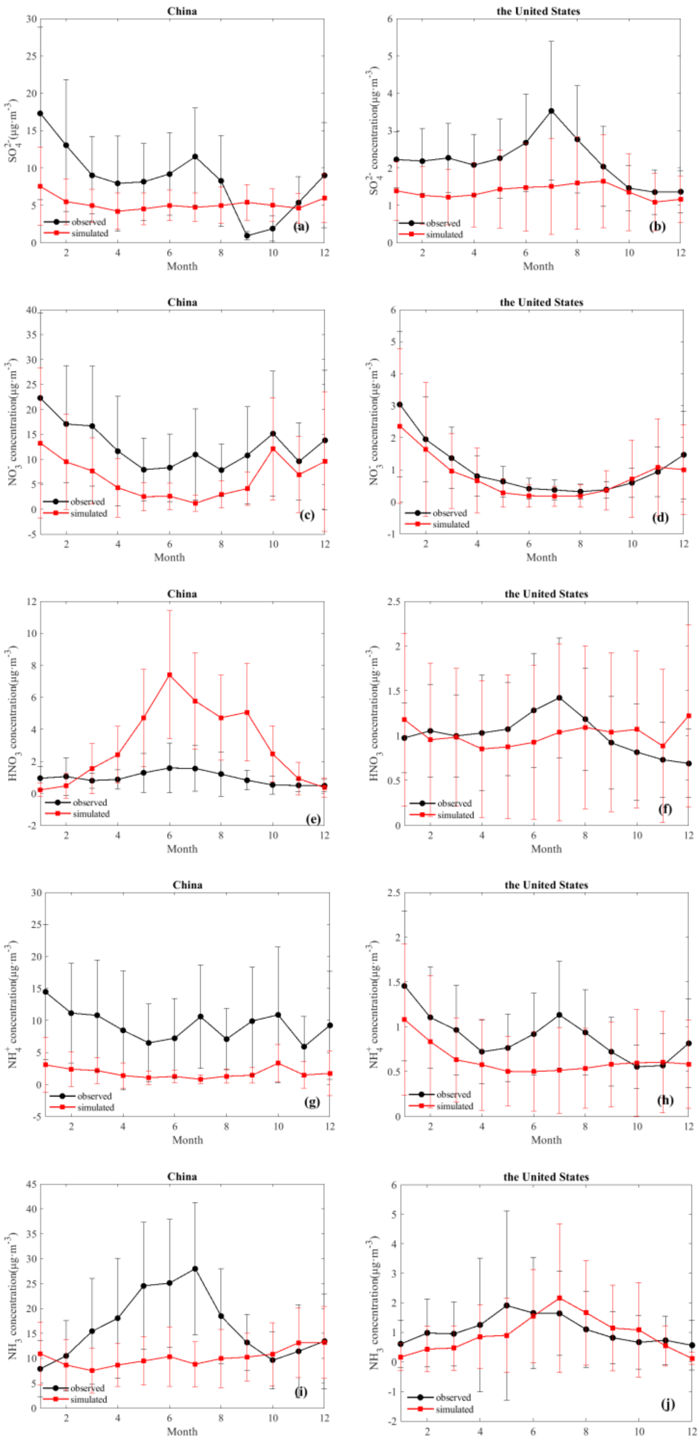

Figure S6: Monthly average concentrations of SO_4^{2-}, NO_3^-, HNO_3^-, NH_4^+, NH_3 : observed versus CMAQ simulated data in China (panels a, c, e, g, i) and in the United States (panels b, d, f, h, j).

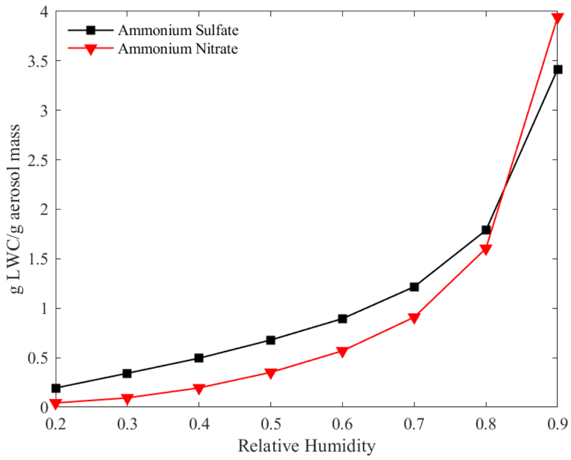

Figure S7: Hygroscopic property of ammonium sulfate and ammonium nitrate represented as the concentration of aerosol liquid water uptake by unit mass of pure aerosol calculated by ISORROPIA-II under metastable condition. This result can be used to illustrate the water uptake ability because the model uses ZSR correlation to calculate water uptake of aerosols which assumes the total concentration of aerosol water equals to the sum of water uptake by each aerosol component(Fountoukis and Nenes, 2007).

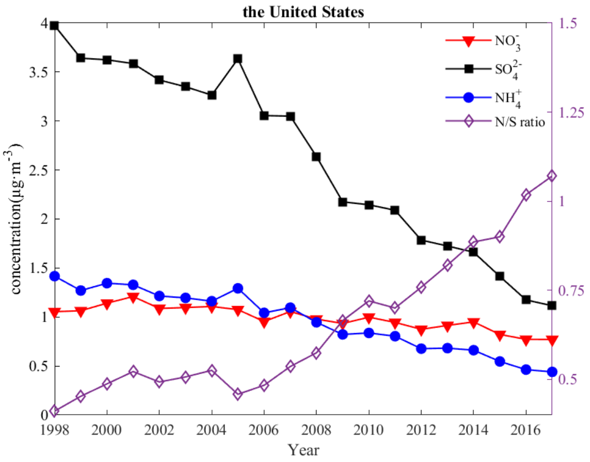

Figure S8: Yearly trend of annual average concentrations NO_3^-, SO_4^{2-} and NH_4^+ observed at the 34 monitoring collocated CASTNET and AMoN sites in the United States.

Table S1: List of the 16 monitoring sites in China

Monitoring Sites in China			
No.	Site name	Latitude	Longitude
1	Chinese Research Academy of Environmental Science（CRAES)	40.04	116.42
2	Anyang	36.09	114.39
3	Baoding	38.87	115.52
4	Dezhou	37.45	116.32
5	Hohhot	40.80	111.64
6	Jinan	36.66	117.05
7	Liulihe	39.58	116.00
8	Qinhuangdao	39.91	119.56
9	Shijiazhuang	38.03	114.54
10	Taiyuan	37.82	112.57
11	Tangshang	39.90	118.60
12	Tianjin	39.10	117.17
13	Xianghe	39.78	116.96
14	Yizhuang	39.80	116.51
15	Yufa	39.52	116.31
16	Zhengzhou	34.28	113.68

Table S2: List of the 34 monitoring sites in the United States.

Monitoring Sites in the United States			
No.	Site name	Latitude	Longitude
1	Parsons	39.09	-79.66
2	Prince Edward	37.17	-78.31
3	Perkinstown	45.21	-90.60
4	Rocky Mtn NP Collocated	40.28	-105.55
5	Sand Mountain	34.29	-85.97
6	Stockton	42.29	-90.00
7	Sequoia NP - Ash Mountain	36.49	-118.83
8	Wash. Crossing	40.31	-74.87
9	Yosemite NP - Turtleback Dome	37.71	-119.71
10	Abington	41.84	-72.01
11	Alhambra	38.87	-89.62
12	Arendtsville	39.92	-77.31
13	Beaufort	34.88	-76.62
14	Caddo Valley	34.18	-93.10
15	Cadiz	36.78	-87.85
16	Chiricahua NM	32.01	-109.39
17	Cherokee Nation	35.75	-94.67
18	Candor	35.26	-79.84
19	Coweeta	35.06	-83.43
20	Connecticut Hill	42.40	-76.65
21	Deer Creek	39.64	-83.26
22	Georgia Station	33.18	-84.41
23	Palo Duro	34.88	-101.67
24	Joshua Tree NP	34.07	-116.39
25	Bondville	40.05	-88.37
26	Great Smoky NP - Look Rock	35.63	-83.94
27	Indian River Lagoon	27.85	-80.46
28	Santee Sioux	42.83	-97.85
29	Beltsville	39.03	-76.82
30	Everglades NP	25.39	-80.68
31	Mount Rainier NP	46.76	-122.12
32	Kane Exp. Forest	41.60	-78.77
33	Konza Prairie	39.10	-96.61
34	Mackville	37.70	-85.05

Table S3: Summary of the inputs of Multivariable Taylor Series Method (MTSM) calculation. The unit of concentrations is μg·m^{-3}, the RH is a relative number with no unit, and the unite of temperature is K. The values in "observation" group are the average values based on observation data, the values in "simulation group" are the average values based on CMAQ simulation data and the "Simulation, population-weighted" group is the population-weighted values based on CMAQ simulation data.

Observation										
	Na^+	TSO_4	TNH_3	TNO_3	TCl	Ca^{2+}	K^+	Mg^{2+}	RH	Temp
China	0.69	9.19	26.53	13.11	4.10	0.03	0.72	0.15	0.45	287.39
US	0.16	2.16	1.87	1.75	0.10	0.03	0.07	0.05	0.71	284.75
Simulation										
	Na^+	TSO_4	TNH_3	TNO_3	TCl	Ca^{2+}	K^+	Mg^{2+}	RH	Temp
China	0.08	1.95	3.05	2.82	0.11	0.05	0.11	0.02	0.72	280.98
US	0.03	0.85	0.56	0.75	0.11	0.02	0.02	0.01	0.72	285.96
Simulation, population-weighted										
	Na^+	TSO_4	TNH_3	TNO_3	TCl	Ca^{2+}	K^+	Mg^{2+}	RH	Temp
China	0.18	3.96	8.41	7.21	0.23	0.09	0.29	0.04	0.70	289.26
US	0.03	1.42	1.79	2.41	0.13	0.03	0.08	0.01	0.66	287.86

Table S4: $PM_{2.5}$, SO_4^{2}, NO_3^- and NH_4^+ concentration and N/S molar ratio collected from other studies in Beijing, Shanghai and Guangzhou. The data in all the cities display an increasing N/S molar ratio along the years.

Location	**Time period**	**Concentration ($\mu g \cdot m^{-3}$)**				**N/S molar ratio**	**Reference**
		$PM_{2.5}$	SO_4^{2-}	NO_3^-	NH_4^+		
Beijing	June-July 2003	131.6	22.6	13.7	9.8	0.94	(Cao et al., 2012)
	March 2005- February 2006	118.5	15.8	7.3	10.1	0.72	(Yang et al., 2011)
	July-August 2005	68.0	22.6	9.9	4.7	0.68	(Pathak et al., 2009)
	January 2013	158.4	16.6	10.3	7.5	0.96	(Liu et al., 2016)
	June 2012-March 2013	112.0	24.2	20.3	15.8	1.30	(Wang et al., 2015)
	April-May 2016	57.0	8.4	12.6	6.7	2.32	(Ding et al., 2019)
	February 2017	60.0	7.3	13.7	7.3	2.91	(Ding et al., 2019)
	July-August 2017	39.0	8.6	9.5	7.2	1.71	(Ding et al., 2019)
	September-October 2017	59.0	6.5	18.5	8.2	4.41	(Ding et al., 2019)
Shanghai	March1999- May 2000	67.7	13	5.8	5.7	0.69	(Yang et al., 2011)
	September-October 2003	96.4	8.7	3.7	3.6	0.66	(Wang et al., 2006)
	July-August 2005	67.0	15.8	7.1	4.1	0.70	(Pathak et al., 2009)
	April 2009-Feburary 2010	94.0	11.7	7.7	4.1	1.02	(Zhao et al., 2015)
	December 2011-November 2012	68.4	12.9	12.6	5.6	1.51	(Zhao et al., 2015)
	2013		14.5	18.0	8.1	1.92	(Ming et al., 2017)
Guangzhou	June-July 2003	39.7	6.4	1.2	1.2	0.30	(Cao et al., 2012)
	October-November 2004	153.9	38.6	8.8	13.6	0.35	(Chang et al., 2013)
	July-August 2005	55.0	13.1	5.2	4.8	0.61	(Pathak et al., 2009)
	June-July 2006	-	6.3	1.3	1.6	0.32	(Huang et al., 2011)
	March-April 2007	-	14.3	7.3	6.1	0.79	(Huang et al., 2011)
	2012	-	8.3	4.6	4.2	0.85	(Liu et al., 2017)

References

Cao, J.-J., Shen, Z.-X., Chow, J. C., Watson, J. G., Lee, S.-C., Tie, X.-X., Ho, K.-F., Wang, G.-H., and Han, Y.-M.: Winter and Summer PM2.5 Chemical Compositions in Fourteen Chinese Cities, Journal of the Air & Waste Management Association, 62, 1214-1226, 10.1080/10962247.2012.701193, 2012.

Chang, S.-Y., Chou, C. C. K., Liu, S., and Zhang, Y.: The Characteristics of PM2.5 and Its Chemical Compositions between Different Prevailing Wind Patterns in Guangzhou, Aerosol and Air Quality Research, 13, 1373-1383, 10.4209/aaqr.2012.09.0253, 2013.

Ding, J., Zhao, P., Su, J., Dong, Q., Du, X., and Zhang, Y.: Aerosol pH and its driving factors in Beijing, Atmos. Chem. Phys., 19, 7939-7954, 10.5194/acp-19-7939-2019, 2019.

Fountoukis, C., and Nenes, A.: ISORROPIA II: a computationally efficient thermodynamic equilibrium model for K^+-Ca^{2+}-Mg^{2+}-NH_4^+-Na^+-SO_4^{2-}-NO_3^--Cl^--H_2O aerosols, Atmos. Chem. Phys., 7, 4639-4659, 10.5194/acp-7-4639-2007, 2007.

Huang, X., Qiu, R., Chan, C. K., and Ravi Kant, P.: Evidence of high PM2.5 strong acidity in ammonia-rich atmosphere of Guangzhou, China: Transition in pathways of ambient ammonia to form aerosol ammonium at [NH4+]/[SO42–]=1.5, Atmospheric Research, 99, 488-495, https://doi.org/10.1016/j.atmosres.2010.11.021, 2011.

Liu, J., Wu, D., Fan, S., Mao, X., and Chen, H.: A one-year, on-line, multi-site observational study on water-soluble inorganic ions in PM2.5 over the Pearl River Delta region, China, Science of The Total Environment, 601-602, 1720-1732, https://doi.org/10.1016/j.scitotenv.2017.06.039, 2017.

Liu, Z., Hu, B., Zhang, J., Yu, Y., and Wang, Y.: Characteristics of aerosol size distributions and chemical compositions during wintertime pollution episodes in Beijing, Atmospheric Research, 168, 1-12, https://doi.org/10.1016/j.atmosres.2015.08.013, 2016.

Ming, L., Jin, L., Li, J., Fu, P., Yang, W., Liu, D., Zhang, G., Wang, Z., and Li, X.: PM2.5 in the Yangtze River Delta, China: Chemical compositions, seasonal variations, and regional pollution events, Environmental Pollution, 223, 200-212, https://doi.org/10.1016/j.envpol.2017.01.013, 2017.

Pathak, R. K., Wu, W. S., and Wang, T.: Summertime $PM_{2.5}$ ionic species in four major cities of China: nitrate formation in an ammonia-deficient atmosphere, Atmos. Chem. Phys., 9, 1711-1722, 10.5194/acp-9-1711-2009, 2009.

Wang, H., Tian, M., Li, X., Chang, Q., Cao, J., Yang, F., Ma, Y., and He, K.: Chemical Composition and Light Extinction Contribution of PM2.5 in Urban Beijing for a 1-Year Period, Aerosol and Air Quality Research, 15, 2200-2211, 10.4209/aaqr.2015.04.0257, 2015.

Wang, Y., Zhuang, G., Zhang, X., Huang, K., Xu, C., Tang, A., Chen, J., and An, Z.: The ion chemistry, seasonal cycle, and sources of PM2.5 and TSP aerosol in Shanghai, Atmospheric Environment, 40, 2935-2952, https://doi.org/10.1016/j.atmosenv.2005.12.051, 2006.

Yang, F., Tan, J., Zhao, Q., Du, Z., He, K., Ma, Y., Duan, F., Chen, G., and Zhao, Q.: Characteristics of PM2.5 speciation in representative megacities and across China, Atmos. Chem. Phys., 11, 5207-5219, 10.5194/acp-11-5207-2011, 2011.

Zhao, M., Qiao, T., Huang, Z., Zhu, M., Xu, W., Xiu, G., Tao, J., and Lee, S.: Comparison of ionic and carbonaceous compositions of PM2.5 in 2009 and 2012 in Shanghai, China, Science of The Total Environment, 536, 695-703, https://doi.org/10.1016/j.scitotenv.2015.07.100, 2015.